

The volume of healthy red blood cells maximizes oxygen transport

Lucas Amoudruz^{a,c}, Athena Economides^{a,b}, and Petros Koumoutsakos^{a,c,*}

^a*Computational Science and Engineering Laboratory, ETH Zürich, CH-8092, Switzerland*

^b*Department of Quantitative Biomedicine, University of Zurich, CH-8057, Switzerland*

^c*School of Engineering and Applied Sciences, Harvard University, Cambridge, MA 02138, United States*

**Corresponding author: petros@seas.harvard.edu*

Abstract

Red blood cells (RBCs) play a crucial role in oxygen transport in living organisms as the vast majority of oxygen in the blood is bound to the hemoglobin molecules in their cytosol. Healthy RBCs have a biconcave shape and a flexible membrane enabling them to undergo substantial reversible elastic deformation as they traverse narrow capillaries during microcirculation. This RBC deformability is critical for efficient circulation while the unique biconcave shape of healthy RBCs is attributed to their specific volume, which affects the amount of oxygen they can carry. However, despite extensive research, the underlying mechanism that determines the optimal RBC volume remains unknown. This paper examines the impact of RBC volume on the efficiency of oxygen transport from a fluid dynamics standpoint. Our investigation reveals that RBCs with volumes similar to those observed in vivo demonstrate superior oxygen transport efficiency in circular tubes similar to arterioles, which represent areas of the circulatory system with the highest flow resistance. Furthermore, we identify mechanisms that impair oxygen transport when the RBC volume deviates from the optimal value. While healthy RBCs produce a maximum cell-free layer thickness that affects flow dissipation, smaller RBC volumes result in greater deformations and thus dissipate more energy. Strikingly, the flow resistance is minimized at the reduced volume of healthy RBCs. Our study highlights that the volume of healthy RBCs maximizes oxygen transport efficiency and may offer insight into developing targeted treatments for circulatory disorders.

Blood flow plays a vital role in sustaining life as it enables the delivery of oxygen and nutrients to every tissue and organ in the body while also removing harmful waste like carbon dioxide. Red blood cells (RBCs) are a crucial component of blood, making up almost half of the total blood volume in humans [31]. These specialized cells are responsible for carrying oxygen from the lungs to the rest of the body, where it is used to fuel cellular metabolism. They are formed by a visco-elastic membrane that surrounds the cytosol of the cell. The cytosol contains a high concentration of hemoglobin, which is responsible for the transportation of oxygen [31, 9]. The RBC membrane is composed of a lipid bilayer anchored to a cytoskeleton and allows for significant deformations [25]. The lipid bilayer of the membrane

behaves like an incompressible liquid crystal with localized bending resistance, while the cytoskeleton provides resistance to local shear and dilation [19]. According to current models, the unstressed shape of the cytoskeleton is an oblate spheroid of reduced volume approximately 0.95, compared to a sphere with the same membrane area [25, 19, 3]. However, at equilibrium healthy RBCs adopt a biconcave shape with a reduced volume (v) of approximately 0.65 [13]. In this paper, we postulate that this volume size is optimal for oxygen transport given a fixed membrane area.

The biconcave shape and reduced volume of RBCs as well as metrics for their optimality remain a subject of debate in the scientific community. Canham [6] suggested that the biconcave shape minimizes

the bending energy of the membrane for a given reduced volume. However, this theory does not explain why RBCs have this particular reduced volume. Some researchers proposed that the biconcave shape allows for a large surface-to-volume ratio for RBCs so that they maximize oxygen exchange between the RBC interior and their environment [24, 38]. The exchange of oxygen between the cytoplasm and the environment is higher for cells with lower thickness because cytoplasmic diffusion may be more limiting than membrane permeability, as shown by Richardson et al. [34]. Other studies suggest that the biconcave shape allows for a more efficient flow through capillaries and kidney tubules due to the RBCs' deformability [25, 30, 39, 29]. Uzoigwe [38] proposed that RBCs have a biconcave shape to maximize their moment of inertia, thereby reducing shear in blood flow and decreasing blood flow resistance in arteries, but did not present any quantitative results. Guo et al. [20] showed that the volume of cells affects their stiffness, while other studies found that osmotic pressure and cell stiffness affect the viscosity of whole blood [37, 36, 32, 35]. Alterations in RBC volume can significantly impact the function of the circulatory system and individual health [38].

In this study, we investigate the hypothesis that the reduced volume of RBCs is optimized for efficient oxygen transport in the circulatory system. To test this hypothesis, we study the transport of a fixed quantity of hemoglobin by RBCs with varying resting shapes parameterized by the reduced volume of the cells. We investigate the effect of the RBC reduced volume on the oxygen flux in a circular tube. This metric has been used experimentally to determine the optimal hematocrit for oxygen transport [36]. We choose a tube with dimensions and pressure gradient similar to those found in arterioles, where flow resistance is highest in the circulatory system [5, 7, 27, 28].

The study relies on a recent and appropriately validated RBC model, comprising visco-elastic membranes enclosing the cytosol and suspended in the blood plasma. The model was extensively calibrated in Amoudruz et al. [3] and validated against experimental data in various flow conditions. The evolution of the solvent and the cytosol are described by dissipative particle dynamics (DPD) [21, 12].

Simulations are performed with *Mirheo*, a high-performance software for blood flow and microfluidics [1].

Results

We examine the flow of RBCs that are suspended within a circular tube with a radius $R = 40 \mu\text{m}$, which is intended to simulate the characteristics of arterioles. The volume fraction of RBCs, or hematocrit, is set to $\text{Ht} = 45\%$ and the blood suspension is subjected to a pressure gradient $\nabla p = 1 \times 10^{-3} \text{cmH}_2\text{O} \mu\text{m}^{-1}$, typical for arterioles of this size [18]. We study different cases with RBC membranes all having the same area and visco-elastic properties but with a different reduced volume $v = V_0/V_s$, where V_0 is the volume of one cell and V_s is that of a sphere with the same area as the cell's membrane. The number of RBCs is adapted to keep the hematocrit constant, $N = \lfloor \pi R^2 \text{LHt}/V_0 \rfloor$. We study a periodic domain with a length $L = 100 \mu\text{m}$ and all quantities are reported for equilibrated flow conditions.

We find that the reduced volume affects the flow patterns and RBCs deformability (fig. 1). Specifically, for low reduced volumes, the cells deform much more than at high values of v . In the limit $v \rightarrow 1$, only spherical cells are allowed, and as the area is constant they cannot deform. RBCs with a healthy reduced volume do not exhibit significant deformations compared to those with lower reduced volumes. Instead, healthy RBCs seem to keep a relatively flat shape similar to tank-treading RBCs.

We quantify the amount of oxygen transport by computing the flux of cytosol in the tube for each value of v ,

$$Q_h = \frac{V_0}{L} \sum_{i=1}^N U_i,$$

where U_i is the time-averaged velocity of the i th RBC's center of mass. We assume that the cytosol contains hemoglobin in equal concentrations for each case so that the flux of cytosol is proportional to the flux of oxygen. Figure 2 shows the flux of cytosol Q_h , normalized by the flux of plasma at $\text{Ht} = 0$,



Figure 1: Snapshots of RBCs flowing near the walls of the tube. The flow direction is from left to right. Cells with different reduced volumes respond differently to flow shear (from left to right: $v = 0.35, 0.65, 0.95$).

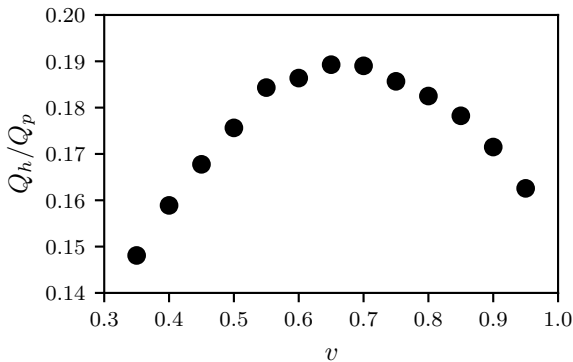


Figure 2: Cytosol flux, normalized by that of the plasma at zero hematocrit, against the reduced volume of RBCs flowing in the tube.

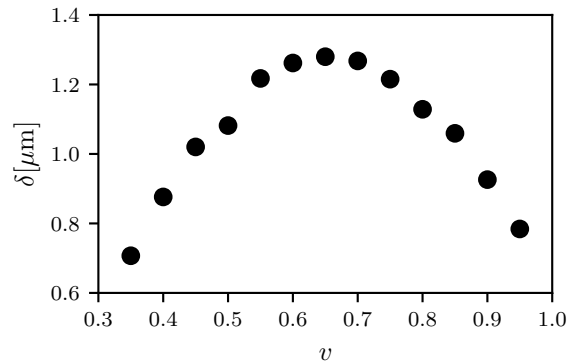


Figure 3: Cell-free layer thickness against the reduced volume of RBCs flowing in the tube.

$Q_p = |\nabla p| \pi R^4 / 8 \eta$, where η is the dynamic viscosity of the plasma, against the reduced volume of the RBCs. In these conditions, Q_h reaches a maximum at a reduced volume $v \approx 0.65$. Strikingly, the flow resistance is minimized at the reduced volume of healthy RBCs.

In order to elucidate the mechanisms that reduce the cytosol flux when the volume of the RBCs deviates from its healthy RBC value, we examine the cell-free layer (CFL) near the walls of the tube. We report its thickness, δ , with respect to the reduced volume v in fig. 3. The larger CFL thickness corresponds to a larger region of high shear rate resulting in a larger flux of hemoglobin (figs. 2 and 3) as the

blood suspension has a larger effective viscosity than pure plasma [8]. Thus, for a given pressure difference, a smaller CFL is responsible for a lower oxygen flux.

We suggest that the change in the CFL thickness depends on the reduced volume of the RBCs. We explain this dependency by observing the deformations of RBCs and their trajectories. The deformation of the cells are quantified by the rim angle (see below) and bending energy of each cell. We distinguish tumbling-like motion due to the external shear stresses, from tank-treading motion, where the membrane rotates around a steady shape. The cell trajectories are quantified by the diffusion coefficient along the azimuth direction.

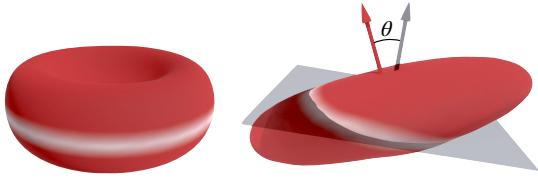


Figure 4: Left: The rim (white) of a RBC at rest. Right: The normal of the rim plane (dark arrow) and the normal of the cell plane (red arrow) form the rim angle θ .

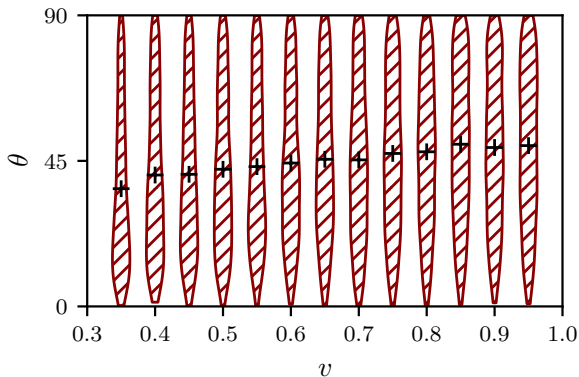


Figure 5: Violin plots illustrating the variation in rim angle distribution θ (in degrees) of flowing cells across different reduced volumes v . Crosses indicate the mean value of θ .

Rim angle

We define the rim angle as the angle between the normal to the principal disc of the cell and that of the region corresponding to the rim of the stress-free state of the cell, see fig. 4 and ref. [11]. For a tumbling RBC, this angle is typically low while for tank-treading RBCs the angle takes values in the whole range, $\theta \in [0, \pi/2]$.

Figure 5 shows the distribution of rim angles θ of cells flowing in the tube for different values of v . On average, the rim angles are smaller at low values of v . Furthermore, the density of θ is more uniform at high values of v than at low reduced volume values.

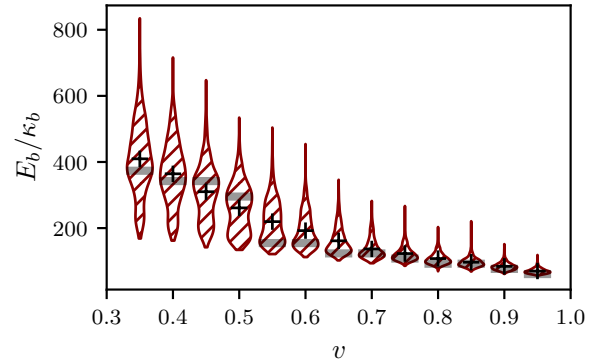


Figure 6: Violin plots illustrating the variation in bending energy distribution of flowing cells across different reduced volumes v . Crosses indicate the mean value of the bending energy while the shaded regions indicate the maximum density. κ_b is the bending modulus.

This suggests that RBCs with a large reduced volume tank-tread while their motion is closer to tumbling at lower values of v .

Bending energy

The deformations of the cells are characterized by the bending energy (eq. (1)). The bending energy of the membrane is high when the cell deforms (e.g. folds) and therefore characterizes complex dynamics and shape changes.

The bending energy distribution of the cells is shown on fig. 6 for different values of v . The mean bending energy decreases with increasing values of v . This is consistent with the fact that the minimum bending energy is achieved for a spherical shape. Nevertheless, we observe differences in the distributions of the bending energies. For $v \geq 0.6$, the bending energies are concentrated close to a minimal value. Instead, when $v < 0.6$, we observe a peak of bending energy well above the minimal values observed at each reduced volume. These high values suggest that RBCs undergo large deformations compared to their resting shape. In particular, we observe cells that are “folding” periodically when v is

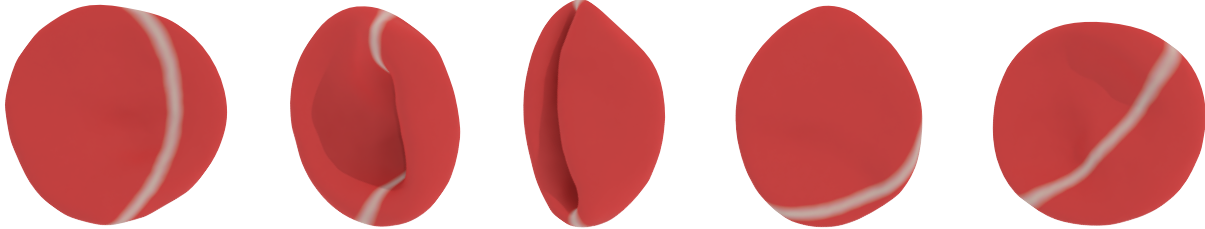


Figure 7: Time sequence of a folding and unfolding RBC (time increasing from left to right). The cell has a reduced volume $v = 0.4$. The white stripe represents the rim of the cell at rest (see fig. 4).

relatively small (fig. 7), as opposed to cells that have a large reduced volume. This mechanism may explain the decrease of the CFL thickness at low values of v . Indeed, when folding or experiencing large deformations, the effective thickness of the RBCs increases and thus the CFL thickness decreases. In addition, the folding of RBCs is accompanied by a high dissipation due to the recirculation of the cytosol inside the cell, which may further decrease the blood flux.

Tank-treading frequency

In linear shear flows, RBCs tank-tread when the shear rate is large enough [16, 10]. The tank-treading frequency (TTF) is reported against the time averaged radial position of the cells on fig. 8. For low values of v , most cells do not tank-tread hence the value estimated for the TTF is low. For larger values of v , the TTF increases linearly with the radial position. This increase is consistent with the nearly linear relationship between the TTF and the shear rate for single cells [16], and assuming that we have a nearly parabolic velocity profile along the radial direction of the tube, hence a linear increase of the shear rate with the radial position r . Furthermore, we observe that the TTF of cells is larger when v increases. This is also expected since spheres in shear flows rotate with a larger frequency than the TTF of RBCs [16]. We suggest that, for relatively thin cells, tank-treading is beneficial for cells to pass each other without deforming and to minimize the effect of their

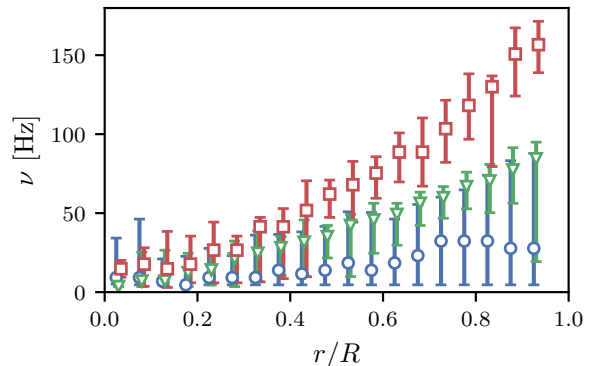


Figure 8: TTF of the RBCs against their time averaged radial position, for $v = 0.4$ (circles), $v = 0.7$ (triangles) and $v = 0.9$ (squares). The symbols and error bars indicate the binned median and the 5% to 95% quantiles, respectively.

collisions, thus contributing to a lower value of δ .

Azimuth diffusion

To characterize the trajectories of the cells, we measure the diffusion coefficient of the cells' positions. Since the RBC suspension is confined along the radial axis of the tube, and the flow is along the tube's axis, we report only the diffusion coefficient of cells along the azimuth direction. The diffusion coefficient is estimated from the mean squared displacement of

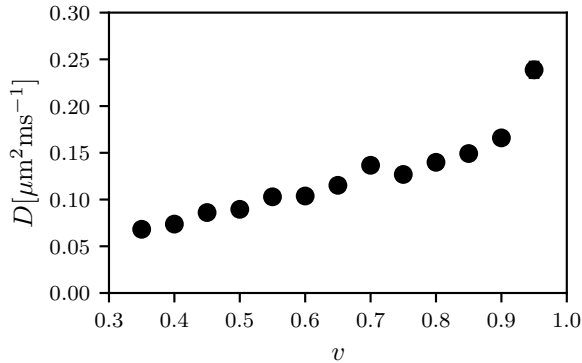


Figure 9: Azimuth diffusion D of the RBCs against the reduced volume v . The error bars correspond to the standard error of D .

the cells along the azimuth direction,

$$D = \lim_{t \rightarrow \infty} \langle l(t)^2 \rangle / 2t, \quad l(t) = \int_{\phi(0)}^{\phi(t)} r d\phi,$$

where r is the radial position of the cell's center of mass and ϕ is the corresponding azimuth angle in cylindrical coordinates. The diffusion coefficient of the cells is reported against v on fig. 9.

The azimuth diffusion increases with the reduced volume of the cells v . We attribute this increase in diffusion to the non-deformability of the cells at high values of v . Indeed, for low values of v the cells can deform enough to avoid migrating perpendicularly to the flow direction when passing each other. In contrast, at high values of v , the cells do not deform, causing the collision with other cells to deviate their trajectories from the flow direction. The collisions, and thus migrations of the cells in the directions perpendicular to the flow, may contribute to reducing the CFL thickness for $v > 0.65$, thus decreasing the transport efficiency of the cytosol.

Discussion

At a physiological hematocrit, the reduced volume of healthy RBCs maximizes the transport of cytosol

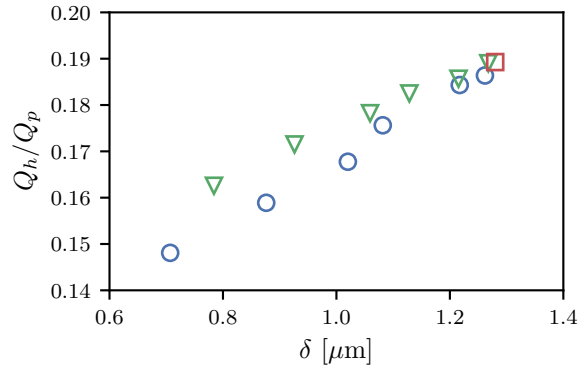


Figure 10: Cytosol flux against the CFL thickness. Circles correspond to cells with $v < 0.65$, triangles those with $v > 0.65$ and the square is for $v = 0.65$.

through relatively large tubes. When the reduced volume of the RBCs deviates from that of healthy cells, we identify two factors that decrease the transport efficiency of oxygen: the change of the CFL thickness, and the dissipation due to the cytosol recirculation and the deformations of the cells.

The viscosity of plasma is smaller than that of whole blood, thus a larger CFL thickness contributes to a higher flux of blood. We find that the CFL thickness is maximized at $v \approx 0.65$. Below this value, cells fold, undergo large deformations and adopt a tumbling rather than tank-treading motion. These deformations increase the effective thickness of the cells along the radial direction, thus reducing the CFL thickness. In contrast, at larger values of v , cells do not deform and have more diffusive trajectories, due to collisions with their neighboring cells. These collisions cause the cells to migrate perpendicularly to the flow direction, thus reducing the CFL thickness. At intermediate values of v , the cells tank-tread, which facilitate their motion relative to each other. This is supported by the shear-thinning behavior of blood when the motion of RBCs transitions from tumbling to tank-treading [15, 17]. The non-spherical shape of healthy RBCs limits the effect of collisions, and they form a maximal CFL thickness.

The CFL thickness alone does not explain the pro-

file observed in fig. 2. Indeed, for the same value of CFL thickness, the cytosol flux is lower for the case with $v < 0.65$ than when $v > 0.65$ (fig. 10). We attribute this difference to the additional dissipation due to the large deformations occurring for cells with smaller reduced volumes. In addition, we expect that tank-treading cells dissipate more energy at lower reduced volumes, as shown for vesicles [23].

We remark that in this study we chose flow conditions corresponding to arterioles, which contribute to the highest flow resistance in the circulatory system. We argue that this trend will remain the same if we sampled a broader range of tube configurations, including large arteries and small capillary vessels. In the latter case, cells with a large reduced volume would not flow due to their large size and would thus have a low oxygen transport efficiency in these conditions. Furthermore we remark that in our study we have neglected the non-uniformity and deformations of the vasculature, the effect of the glycocalyx, the variability of the membrane visco-elastic properties and the pressure waves due to heart beats. While we do not expect major qualitative changes, the effect of these perturbations will be the subject of further research.

Summary

We demonstrate, through high fidelity simulations, that RBCs with volumes similar to those observed in vivo optimize the efficiency of oxygen transport in circular tubes similar to arterioles. We deploy high fidelity simulations of a thoroughly validated RBC model in flow conditions close to those found in arterioles, where the vascular resistance is maximal. We qualitatively explain the variation of oxygen transport efficiency with respect of the reduced volume of the cells based on the CFL thickness and the dissipation due to the cells deformability. At low reduced volumes, cells deform and fold, thus occupy a larger effective volume on average. This causes the CFL thickness to decrease. In addition, the deformations of cells induces large dissipation due to the recirculation of the cytosol. At large reduced volumes, cells collide and migrate in the directions perpendicular to

the flow. These trajectories also contribute to reducing the CFL thickness and thus the oxygen transport is lower.

The present findings provide valuable insights into the mechanisms of oxygen transport in the body and could potentially have significant implications for the advancement of therapies aimed at treating circulatory disorders.

Methods

Blood Model

We model blood with RBCs's composed of visco-elastic membranes surrounding their viscous cytosol, and suspended in the blood plasma. The RBC membrane deforms from forces that arise from bending resistance of the lipid-bilayer, as well as due to the shear and dilation elasticity of the cytoskeleton with respect to its stress-free state (SFS), and membrane viscosity. The resistance to bending is described by the energy :

$$U_{bending} = 2\kappa_b \oint H^2 dA, \quad (1)$$

where the integral is taken over the membrane surface, κ_b is the bending modulus and H is the local mean curvature. The in-plane elastic energy is given by

$$U_{in-plane} = \frac{K_\alpha}{2} \oint (\alpha^2 + a_3\alpha^3 + a_4\alpha^4) dA_0 + \mu \oint (\beta + b_1\alpha\beta + b_2\beta^2) dA_0,$$

where the integral is taken over the SFS surface, α and β are the local dilation and shear strain invariants, respectively, K_α is the dilation elastic modulus, μ is the shear elastic modulus and the coefficients a_3 , a_4 , b_1 and b_2 are parameters that control the non-linearity of the membrane elasticity for large deformations [26].

In the present model the membrane is composed of particles located at the corners of a triangulated mesh and evolve according to Newton's law of motion. The bending energy is discretized following references [22, 4], and the in-plane energy is computed

Parameter	Value
κ_b	$2.10 \times 10^{-19} \text{ J}$
μ	$4.99 \mu\text{N m}^{-1}$
K_α	$4.99 \mu\text{N m}^{-1}$
a_3	-2
a_4	8
b_1	0.7
b_2	1.84
η_m	$0.42 \times 10^{-6} \text{ Pa s m}$
A_0	$135 \mu\text{m}^2$
V_0	varying
k_A	0.5 J/m^2
k_V	$7.23 \times 10^5 \text{ J/m}^3$

Table 1: Parameters of the RBC model.

as described in Lim et al. [25]. The forces acting on the particles are the negative gradients of the discretized energy terms, with respect to the particle positions. Dissipation on the membrane is modeled by particles sharing an edge in the triangle mesh that exert a pairwise force as described in Fedosov [14], proportional to the membrane viscosity η_m . Finally, the area of the membrane and the volume of the cytosol are constrained through energy penalization terms,

$$U_{area} = k_A \frac{(A - A_0)^2}{A_0}, \quad U_{volume} = k_V \frac{(V - V_0)^2}{V_0},$$

where A_0 and V_0 are the area and volume of the cell at rest and A and V are the area and volume of the cell, respectively. The values of the RBC parameters are listed in table 1.

The RBC cytosol and surrounding plasma are represented with particles that evolve through DPD interactions [21, 12, 3]. We emphasize that the model parameters are selected so as to correspond to the 1:5 ratio of viscosities for the plasma and the RBC cytosol. To model the no-slip and no-through boundary conditions on walls, particles are bounced-back and interact with frozen particles through DPD interactions [33]. In addition, DPD particles are bounced-back from membrane surfaces, with conservation of momentum, and interact with the membrane particles through the dissipative and stochastic parts of the DPD interactions [14]. The cytosol and plasma

particles interact with each other only through the conservative part of the DPD forces. The DPD parameters are chosen as described in [2].

Computation of the TTF

The TTF is estimated by computing the Fourier transform of the rim angle time series of each cell and selecting the frequency of the largest mode, divided by 2 since the rim angle of a tank-treading cell undergoes 2 revolutions per tank-treading revolution. Note that we exclude cells having an average rim angle $\bar{\theta}$ larger than $\pi/4$, and the tumbling cells, which we characterize by $\bar{\theta} < \pi/8$.

Acknowledgments

We would like to thank Xin Bian for the idea of using the rim angle to perform the analysis. We acknowledge the computational resources granted by the Swiss National Supercomputing Center (CSCS) under the project ID “s929”.

References

- [1] Dmitry Alexeev, Lucas Amoudruz, Sergey Litvinov, and Petros Koumoutsakos. Mirheo: High-performance mesoscale simulations for microfluidics. *Computer Physics Communications*, 254:107298, 2020.
- [2] Lucas Amoudruz. *Simulations and Control of Artificial Microswimmers in Blood*. PhD thesis, ETH Zurich, 2022.
- [3] Lucas Amoudruz, Athena Economides, Georgios Arampatzis, and Petros Koumoutsakos. The stress-free state of human erythrocytes: Data-driven inference of a transferable RBC model. *Biophysical Journal*, 122(8):1517–1525, apr 2023.
- [4] Xin Bian, Sergey Litvinov, and Petros Koumoutsakos. Bending models of lipid bilayer membranes: Spontaneous curvature

- and area-difference elasticity. *Comput. Method. Appl. M.*, 359:112758, feb 2020.
- [5] H Glenn Bohlen, Robert W Gore, and Phillip M Hutchins. Comparison of microvascular pressures in normal and spontaneously hypertensive rats. *Microvascular research*, 13(1):125–130, 1977.
- [6] Peter B Canham. The minimum energy of bending as a possible explanation of the biconcave shape of the human red blood cell. *Journal of theoretical biology*, 26(1):61–81, 1970.
- [7] WILLIAM M Chilian, CHARLES L Eastham, and MELVIN L Marcus. Microvascular distribution of coronary vascular resistance in beating left ventricle. *American Journal of Physiology-Heart and Circulatory Physiology*, 251(4):H779–H788, 1986.
- [8] Giles R Cokelet and Harry L Goldsmith. Decreased hydrodynamic resistance in the two-phase flow of blood through small vertical tubes at low flow rates. *Circulation research*, 68(1):1–17, 1991.
- [9] Giuseppe Di Caprio, Chris Stokes, John M Higgins, and Ethan Schonbrun. Single-cell measurement of red blood cell oxygen affinity. *Proceedings of the National Academy of Sciences*, 112(32):9984–9989, 2015.
- [10] Jules Dupire, Marius Socol, and Annie Vialat. Full dynamics of a red blood cell in shear flow. *Proceedings of the National Academy of Sciences*, 109(51):20808–20813, 2012.
- [11] Eva Athena Economides. *Data informed, predictive simulations of blood microfluidics*. PhD thesis, ETH Zurich, 2020.
- [12] Pep Espanol and Patrick Warren. Statistical mechanics of dissipative particle dynamics. *EPL (Europhysics Letters)*, 30(4):191, 1995.
- [13] Evan Evans and Yuan Cheng Fung. Improved measurements of the erythrocyte geometry. *Microvascular Research*, 4(4):335–347, 1972.
- [14] Dmitry A Fedosov. *Multiscale modeling of blood flow and soft matter*. PhD thesis, Citeseer, 2010.
- [15] Dmitry A Fedosov, Wenxiao Pan, Bruce Caswell, Gerhard Gompper, and George E Karniadakis. Predicting human blood viscosity in silico. *Proceedings of the National Academy of Sciences*, 108(29):11772–11777, 2011.
- [16] Thomas M Fischer. Tank-Tread Frequency of the Red Cell Membrane : Dependence on the Viscosity of the Suspending Medium. *Biophysical Journal*, 93(7):2553–2561, 2007.
- [17] Alison M Forsyth, Jiandi Wan, Philip D Owrutsky, Manouk Abkarian, and Howard A Stone. Multiscale approach to link red blood cell dynamics, shear viscosity, and atp release. *Proceedings of the National Academy of Sciences*, 108(27):10986–10991, 2011.
- [18] Yuan-Cheng Fung. Biomechanics: circulation. *Shock*, 9(2):155, 1998.
- [19] Nadeeshani Maheshika Geekiyanage, Marie Anne Balanant, Emilie Sauret, Suvasih Saha, Robert Flower, Chwee Teck Lim, and YuanTong Gu. A coarse-grained red blood cell membrane model to study stomatocyte-discocyte-echinocyte morphologies. *PLoS One*, 14(4):e0215447, 2019.
- [20] Ming Guo, Adrian F Pegoraro, Angelo Mao, Enhua H Zhou, Praveen R Arany, Yulong Han, Dylan T Burnette, Mikkel H Jensen, Karen E Kasza, Jeffrey R Moore, et al. Cell volume change through water efflux impacts cell stiffness and stem cell fate. *Proceedings of the National Academy of Sciences*, 114(41):E8618–E8627, 2017.
- [21] PJ Hoogerbrugge and JMVA Koelman. Simulating microscopic hydrodynamic phenomena with dissipative particle dynamics. *EPL (Europhysics Letters)*, 19(3):155, 1992.
- [22] Frank Jülicher. The morphology of vesicles of higher topological genus: conformal degeneracy

- and conformal modes. *Journal de Physique II*, 6(12):1797–1824, 1996.
- [23] Martin Kraus, Wolfgang Wintz, Udo Seifert, and Reinhard Lipowsky. Fluid vesicles in shear flow. *Physical Review Letters*, 77(17):3685–3688, 1996.
- [24] JG Lenard. A note on the shape of the erythrocyte. *Bulletin of Mathematical Biology*, 36(1):55–58, 1974.
- [25] Gerald Lim H. W., Michael Wortis, and Ranjan Mukhopadhyay. Red Blood Cell Shapes and Shape Transformations: Newtonian Mechanics of a Composite Membrane. *Soft Matter*, 4, 2008.
- [26] Gerald Lim HW, Michael Wortis, and Ranjan Mukhopadhyay. Stomatocyte–discocyte–echinocyte sequence of the human red blood cell: Evidence for the bilayer–couple hypothesis from membrane mechanics. *Proceedings of the National Academy of Sciences*, 99(26):16766–16769, 2002.
- [27] Gerald A Meininger. Responses of sequentially branching macro-and microvessels during reactive hyperemia in skeletal muscle. *Microvascular research*, 34(1):29–45, 1987.
- [28] MJ Mulvany and C Aalkjaer. Structure and function of small arteries. *Physiological reviews*, 70(4):921–961, 1990.
- [29] Arman Namvar, Adam J Blanch, Matthew W Dixon, Olivia MS Carmo, Boyin Liu, Snigdha Tiash, Oliver Looker, Dean Andrew, Li-Jin Chan, Wai-Hong Tham, et al. Surface area-to-volume ratio, not cellular viscoelasticity, is the major determinant of red blood cell traversal through small channels. *Cellular microbiology*, 23(1):e13270, 2021.
- [30] Igor V Pivkin, Zhangli Peng, George E Karniadakis, Pierre A Buffet, Ming Dao, and Subra Suresh. Biomechanics of red blood cells in human spleen and consequences for physiology and disease. *Proceedings of the National Academy of Sciences*, 113(28):7804–7809, 2016.
- [31] Aleksander S Popel. Theory of oxygen transport to tissue. *Critical reviews in biomedical engineering*, 17(3):257, 1989.
- [32] WH Reinhart, M Singh-Marchetti, and PW Straub. The influence of erythrocyte shape on suspension viscosities. *European journal of clinical investigation*, 22(1):38–44, 1992.
- [33] M Revenga, I Zuniga, P Espanol, and I Pagonabarraga. Boundary models in dpd. *International Journal of Modern Physics C*, 9(08):1319–1328, 1998.
- [34] Sarah L Richardson, Alzbeta Hulikova, Melanie Proven, Ria Hipkiss, Magbor Akanni, Noémi BA Roy, and Pawel Swietach. Single-cell o2 exchange imaging shows that cytoplasmic diffusion is a dominant barrier to efficient gas transport in red blood cells. *Proceedings of the National Academy of Sciences*, 117(18):10067–10078, 2020.
- [35] H Schmid-Schönbein and RE Wells Jr. Rheological properties of human erythrocytes and their influence upon the “anomalous” viscosity of blood. In *Ergebnisse der Physiologie Reviews of Physiology, Volume 63*, pages 146–219. Springer, 2010.
- [36] HO Stone, HK Thompson Jr, and K Schmidt-Nielsen. Influence of erythrocytes on blood viscosity. *American Journal of Physiology-Legacy Content*, 214(4):913–918, 1968.
- [37] Max M Strumia, Martha Phillips, Albert B Sample, M Elizabeth Burns, and Pasquale Mariano. Effect of red cell factors on the relative viscosity of whole blood. *American Journal of Clinical Pathology*, 39(5):464–474, 1963.
- [38] Chika Uzoigwe. The human erythrocyte has developed the biconcave disc shape to optimise the flow properties of the blood in the large vessels. *Medical hypotheses*, 67(5):1159–1163, 2006.
- [39] Koohyar Vahidkhah, Peter Balogh, and Prosenjit Bagchi. Flow of red blood cells in stenosed microvessels. *Scientific reports*, 6(1):1–15, 2016.